

Zero temperature solutions of the Edwards-Anderson model in random Husimi lattices

Alejandro Lage-Castellanos* and Roberto Mulet†
*Henri-Poincaré Group of Complex Systems, Physics Faculty,
University of Havana, La Habana, CP 10400, Cuba and
Department of Theoretical Physics, Physics Faculty,
University of Havana, La Habana, CP 10400, Cuba*
(Dated: August 13, 2021)

We solve the Edwards-Anderson model (EA) in different Husimi lattices using the cavity method at replica symmetric (RS) and 1-step of replica symmetry breaking (1RSB) levels. We show that, at $T = 0$, the structure of the solution space depends on the parity of the loop sizes. Husimi lattices with odd loop sizes may have a trivial paramagnetic solution thermodynamically relevant for highly frustrated systems while, in Husimi lattices with even loop sizes, this solution is absent. The range of stability under 1RSB perturbations of this and other RS solutions is computed analytically (when possible) or numerically. We also study the transition from 1RSB solutions to paramagnetic and ferromagnetic RS solutions. Finally we compare the solutions of the EA model in Husimi lattices with that on the (short loops free) Bethe lattices, showing that already for loop sizes of order 8 both models behave similarly.

PACS numbers: 75.10.Nr, 75.40.Cx, 05.70.Fh, 64.60.aq

I. INTRODUCTION

Spin glasses are among the most complex problems in Statistical Mechanics. During the 80's a lot of effort was devoted to the subject, see for example [1] for a comprehensive collection of relevant works during this decade. It was soon realized that the difficulties in finding an analytical solution to these problems depend strongly on the topology of the interactions between the variables [1, 2]. For example, in fully connected systems, in which each variable interacts with all the others, a compact solution may be found using the Parisi ansatz[1, 3, 4]. On the other hand, the situation for finite connectivity (FC) systems is far more complicated. The main difficulty is the appearance, after a standard replica calculation of an infinite number of overlaps[2, 5]. Therefore, for many years only Replica Symmetric or variational solutions were known for these models.

The importance of finite connectivity systems is twofold: first, one may hope to get a better understanding of finite dimensional systems, since (FC) models include the notion of neighborhood, a concept that is absent in fully-connected systems. Second, there is a clear connection between finite connectivity systems and many constraint satisfaction problems. For example, the K-sat [6], the coloring [7], the traveling salesman [8] and the vertex cover [9, 10] problems turn out to have a finite connectivity structure.

A few years ago, Mezard and Parisi[11, 12] generalized a technique already known as the cavity method[13] to deal with systems with many pure states. This generalization permitted, for the first time in FC systems, the formal introduction of replica symmetry breaking at different levels. Although, it is worth reminding that even the one-Step Replica Symmetry Breaking solution (1RSB) involves as an order parameter a functional distribution.

Moreover, thanks to the aforementioned strong connection between finite connectivity spin systems and many constraint-satisfaction problems[14] this approach sheds some light on the characteristics of the solution space of some of these problems [6, 7, 9, 10], (see also [15, 16] for recent developments in this field). In addition, this cavity method, inspired a novel message-passing algorithm to deal with single instances of several combinatorial problems [17, 18, 19]. Unfortunately, the occurrence of short loops in finite connectivity graphs introduces strong correlations among neighboring sites and in this case, the hypothesis behind the cavity method may be violated. As a consequence, message-passing algorithms usually fail when short loops are present[20, 21, 22, 23]. On the other hand, fully understanding the role of short loops in the energy landscape of finite dimensional spin glasses remains an elusive task[24, 25].

To gain some insight about these problems, we think that it is convenient to look at the properties of a spin glass model, where the hypothesis behind the cavity approximation remain valid, but where the influence of short loop

*Electronic address: ale.lage@gmail.com

†Electronic address: mulet@fisica.uh.cu

structures may be analyzed in detail. Then, we choose to study the ground state characteristics of the Edwards-Anderson model in a Husimi graph. The tree-like structure of the Husimi lattice allows the use of the machinery behind the cavity method, and at the same time, we may tune the loop sizes and the connectivity of the graph to discover their influence on the zero temperature energy landscape of the model.

The paper is organized as follows: In section II we introduce the model, the self-consistent cavity equations that solve it and the definition of the relevant physical quantities. Then, in section III we show closed analytical results for the triangular Husimi lattice. In section IV appears the analysis of more general lattices and finally in section V we present the conclusions of the work.

II. THE MODEL AND THE CAVITY SOLUTION

A Husimi *tree* is formally “a connected graph where no bond (edge) lies in more than one cycle”. It can be visualized as a tree made out of loops, as shown in figure 1. A Husimi tree is called *pure* if all the loops have the same length. It is also called *regular* if all the vertexes belong to the same number of loops [26]. On the other hand, the Husimi *lattice* (also Husimi *graph*) is a graph that looks locally like a Husimi tree, but where large loops are present. It is a random hyper-graph in the sense that by taking the short loops of the Husimi tree as building units, we define the ensemble of pure and regular Husimi graphs as the ensemble of all graphs in which the vertexes belong to $K + 1$ short loops of the same length $c + 1$.

For example, the simplest (and trivial) Husimi tree is the one in which $c = 1$ and coincides with a Cayley tree. The simplest Husimi lattice, $c = 1$ coincides with the Bethe lattice defined in [11]. The simplest, non-trivial, case of a Husimi lattice has $c = 2$, (a triangle) and $K = 1$, each vertex is shared by two triangles (see figure 1). The generalization to more complex structures is straightforward, for example, either c or K or both may be taken as random variables such that the local structure of the graph changes from site to site. Here we consider the ensemble of pure and regular Husimi graphs, meaning that all short loops have the same length, and that all vertexes belong to the same number of (short) loops.

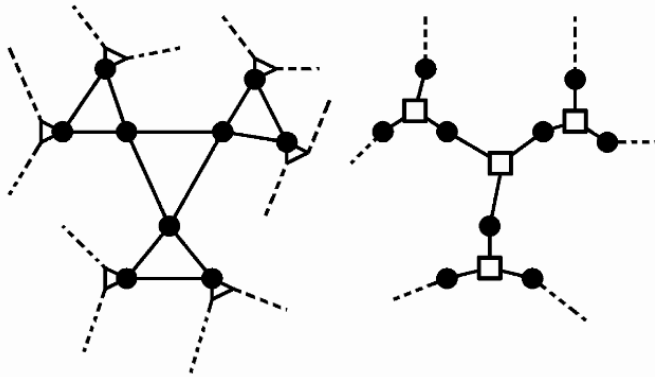


FIG. 1: Left: schematic representation of a representative part of a Husimi graph with $c = 2$ (triangle) and $K = 1$. Right: factor graph representation of the same Husimi lattice. In the factor graph representation, $c + 1$ is the degree of factor nodes (white squares), while $K + 1$ is the degree of nodes (black circles).

In this work we study, using the cavity method at zero temperature [12], the ground state properties of the Edwards-Anderson model in an average Husimi graph. The Edwards-Anderson model is defined by the Hamiltonian:

$$\mathcal{H} = - \sum_{\langle i,j \rangle} J_{i,j} S_i S_j \quad (1)$$

where $\langle i, j \rangle$ stands for the nearest neighbors in the graph, $S_i = \pm 1$ are Ising variables located at the vertexes, and the bonds represent random exchange couplings $J_{i,j}$. The couplings are taken from the distribution:

$$P(J) = \frac{1 + \rho}{2} \delta(J - 1) + \frac{1 - \rho}{2} \delta(J + 1) \quad (2)$$

where $\rho \in [-1, 1]$ parameterizes the bias between ferromagnetic and anti-ferromagnetic interactions. If $\rho = 1(-1)$ the system is purely ferromagnetic (anti-ferromagnetic), and if $\rho = 0$ the system is unbiased.

As will be discussed in more detail below, the cavity method may be easily written in term of messages between Husimi *loops* and sites. The idea is to use a factor graph that considers all the interactions around a loop as a single function node (see figure 1), then inheriting the tree-like structure of the Husimi graph at the loop level. We will use the cavity method at two levels of approximations: the replica symmetric approximation (RS) and the one step replica symmetry breaking approximation (1RSB). It will turn out that depending on c , K and ρ , either the RS approximation or the 1RSB are more appropriate to describe the ground state of the system. We leave for future works the analysis of the stability of the 1RSB solution.

A. The Self-Consistent Cavity Equations at $T = 0$

In order to write the cavity equations for the model, it is convenient to define the problem using a factor graph representation. A factor graph[27] is a bipartite graph in which one subset of the nodes represents local interactions while the other subset represents variables. In this case, it is reasonable to assume that each loop, a , corresponds to a function node, and each site, i to a variable node (see figure 1). With this notation, equation (1) may be written as a sum of loop contributions $\mathcal{H} = \sum_a H_a$ where:

$$H_a = - \sum_i^{c+1} J_{i,i+1} S_i S_{i+1} \quad (3)$$

where we assumed periodic boundary conditions in the index i within the loop.

Then, since the resulting bipartite graph shares the structure of the Husimi lattice, it is locally tree-like and one expects the convergence of the cavity equations below.

1. Replica Symmetric equations

The self-consistent cavity equations in the Husimi lattice may be derived following the approach in [12]. Let us consider a set of c cavity spins $S_1 \dots S_c$ each of which belongs to K loops and receives a field h_i from the interactions with these loops. The iteration procedure consists in adding a new spin S_0 to the cavity graph together with $c + 1$ couplings $J_{i,i+1}$, forming a loop (a function node) between all the c cavity spins and the spin S_0 . With this new loop, the cavity spins $S_1 \dots S_c$ complete their $K + 1$ loops, and a field contribution $u_{a \rightarrow 0}$, that can be computed from the values of $h_1 \dots h_c$ and $J_{0,1} \dots J_{c,0}$, appears on spin S_0 :

$$\begin{aligned} u_{a \rightarrow 0} = \hat{u}(\underline{J}, \underline{h}) &= \sum_{S_0} S_0 \min_{S_1 \dots S_c} H_a \\ &= -\frac{1}{2} \sum_{S_0} S_0 \max_{S_1 \dots S_c} \{J_{0,1} S_0 S_1 + \sum_{i=1}^{c-1} (J_{i,i+1} S_i S_{i+1} + h_i S_i) + h_c S_c + J_{c,0} S_c S_0\} \end{aligned} \quad (4)$$

Then, the cavity field in the spin S_0 is $h_0 = \sum_{a=1 \dots K} u_a$ where all u_a are computed independently by the cavity iteration described above. The u are called cavity messages or biases, and can be interpreted as the contribution of a given loop a to the cavity field in S_0 . The cavity fields $h_1, h_2, \dots h_c$ entering a loop, will be referred from now on as \underline{h} for notation clarity. Similarly \underline{J} will stand for the set of all the $c + 1$ coupling constants, $J_{i,j}$, of the function node. Equation (4) is nothing but the difference between the minimum energy configuration of the spins at the loop when the cavity spin S_0 is up and down. Following equation (4) it is easy to prove that independently of c and K the cavity messages in this model take only integer values: $u \in \{-2, -1, 0, 1, 2\}$.

Furthermore, it is expected that the distribution of these fields is stable during the iteration procedure[12]. This consideration yields the self-consistent cavity equations for the fields distribution $\mathcal{P}(h)$ and the messages distribution $\mathcal{Q}(u)$:

$$\mathcal{P}(h) = \int \delta(h - \sum_a u_a) \prod_{a=1}^K d\mathcal{Q}(u_a) \quad (5)$$

$$\mathcal{Q}(u) = E_J \int \delta(u - \hat{u}(\underline{J}, \underline{h})) \prod_{i=1}^c d\mathcal{P}(h_i) \quad (6)$$

$\mathcal{P}(h)$ and $\mathcal{Q}(u)$ are distributions of fields and biases that represent the probability of finding a field or bias in any site of the graph and E_J is an average over the $J_{i,j}$. These two equations can be folded into one that is equivalent to the ‘‘Parent to Child’’ messages-passing algorithm described in [20] for single instances:

$$\mathcal{Q}(u) = E_J \int \delta(u - \hat{u}(\underline{J}, \sum_{i=1}^K u_i)) \prod_{i=1}^{cK} d\mathcal{Q}(u_i) \quad (7)$$

This is a self-consistent equation for the RS order parameter $\mathcal{Q}(u)$. As the biases are integers $u \in \{-2, -1, 0, 1, 2\}$, $\mathcal{Q}(u)$ can be parameterized with five numbers $p_{-2}, p_{-1}, p_0, p_1, p_2$:

$$\mathcal{Q}(u) = p_{-2}\delta_{u,-2} + p_{-1}\delta_{u,-1} + p_0\delta_{u,0} + p_1\delta_{u,1} + p_2\delta_{u,2} \quad (8)$$

(or four if we consider the normalization constraint) that represent the probabilities p_u of finding a message u going from a function node to a site.

With the help of (8) the self-consistent equation (7) may be written as a set of five equations relating the parameters $p_{-2}, p_{-1}, p_0, p_1, p_2$. Then, the right-hand side of (7) constitutes a sum of terms of degree $c \cdot K$ in the probabilities p , and degree $c + 1$ in ρ . These equations are highly coupled and non-linear: all 5^{cK} combinations of fields and 2^{c+1} combinations of couplings have to be considered. While in some cases one is able to find analytical solutions for all ρ , in more general situations equation (7) must be solved numerically.

Once the RS solution $\mathcal{Q}_{RS}(u)$ of the self-consistent equation (7) for a given ρ is known, this can be used to compute the expected value of the energy in the graph, as:

$$U = -\frac{K+1}{c+1} E_J \int \hat{a}(\underline{J}, \sum_{i=1}^K u_i) \prod_{i=1}^{cK} d\mathcal{Q}(u_i) + \frac{(Kc-1)}{c+1} \int |\sum u_i| \prod_{i=1}^{k+1} d\mathcal{Q}(u_i) \quad (9)$$

where the function $\hat{a}(\cdot)$ is an energetic term very similar to the function $\hat{u}(\cdot)$:

$$\hat{a}(\underline{J}, \underline{h}) = -\frac{1}{2} \sum_{S_0} \max_{S_1 \dots S_c} \{J_{0,1} S_0 S_1 + \sum_{i=1}^{c-1} (J_{i,i+1} S_i S_{i+1} + h_i S_i) + h_c S_c + J_{c,0} S_c S_0\} \quad (10)$$

and is exactly the energy gained by the local state of the graph when the spin S_0 is added to the cavity in the iteration procedure.

The RS solution is valid if the system has a single pure state. In the more general case in which the system has many pure states it usually fails. The reason is that within the RS approximation one assumes that under the process of iteration the ground states of the graphs with N and $N + 1$ spins are related. This is not necessary true[12], and in such cases one must go beyond the RS solution to the 1RSB approximation. Another, perhaps, more numerical intuition is that running the message-passing algorithm, i.e. equation (7), over a single graph one observes that the RS equations have multiple fixed points, which is a signature of the appearance of multiple stationary states for the system[16].

2. 1RSB equations

The 1RSB cavity method assumes that there exists an exponential number $\mathcal{N}(\epsilon) \sim \exp(N\Sigma(\epsilon))$ of pure states[1, 12] with intensive energy $\epsilon = E^\alpha/N$, characterized by the complexity function $\Sigma(\epsilon)$. In this case the correct description of the interaction between a loop (node) and a spin is not given by a single message u , but by a distribution $Q(u)$ representing all different messages in all pure states, and the correct order parameter is now the functional $\mathcal{Q}[Q(u)]$ defining the probability of finding a distribution $Q(u)$ in a randomly selected node of the graph. The hypotheses made for the RS approximation are valid in each pure state α , but the statistics are more subtle, since the ground state can move from one pure state to another when the iteration procedure is carried out [11, 12]. The self-consistent equation for the new order parameter is similar to the RS equation for $\mathcal{Q}(u)$:

$$\mathcal{Q}[Q] = E_J \int \delta^{(F)}(Q - \hat{Q}[\underline{J}, \underline{Q}_i]) \prod_{a=1}^{cK} d\mathcal{Q}[Q_a] \quad (11)$$

where \underline{Q}_a represents the set of all the cK distributions Q_a in the cavity iteration procedure. The functional delta accounts for the iteration of messages, and is defined by:

$$\hat{Q}[\underline{J}, \underline{Q}_a](u) = \frac{1}{A[\underline{J}, \underline{Q}_a]} \int e^{\mu \hat{a}(\underline{J}, \underline{\Sigma}^K u)} \delta(u - \hat{u}(\underline{J}, \underline{\Sigma}^K u)) \prod_{a=1}^{cK} dQ_a(u_a) \quad (12)$$

where the exponential Boltzmann factor is the so called ‘‘re-weighting’’ that takes into account the energy shifts between states when the iteration procedure is carried out [12]. Note that the function $\hat{a}(\cdot)$ was already defined in eq. (10).

In short, in the 1RSB approximation each of the states appears with a weight proportional to $e^{-\mu f}$ where this μ plays the role of an inverse temperature and f is the corresponding free energy of the state[11]. In the replica language the parameter μ stands for the product of the Parisi’s replica parameter m and the inverse temperature β in the zero temperature limit[11, 12]. The term $A[\underline{J}, \underline{Q}_a]$ is a normalization constant given by:

$$A[\underline{J}, \underline{Q}_a] = \int e^{\mu \hat{a}(\underline{J}, \underline{\Sigma}^K u)} \prod_a^{cK} dQ_a(u) \quad (13)$$

and can be thought as a local partition function.

The order parameter $\mathcal{Q}_{1RSB}[Q]$ solution of equation (11) can be rarely found analytically, and furthermore, it depends on the variational parameter μ . The 1RSB solution, then, is quite more involved than the RS one, not only because the order parameter becomes a functional, but also because this functional has to be found numerically, and extremized over the parameter μ , as is explained next.

3. Free energy, energy and complexity

Within the 1RSB cavity formalism[11, 12], a generalized free energy, $\phi(\mu)$, can be defined as :

$$\phi(\mu) = \langle \phi_{site}(\mu) \rangle - \frac{(K+1)c}{c+1} \langle \phi_{node}(\mu) \rangle \quad (14)$$

where the $\phi_{node}(\mu)$ is the contribution from the loops and $\phi_{site}(\mu)$ is the contribution coming from individual sites in the Husimi graph. The previous expression for $\phi(\mu)$ reduces to the one in [12] for the EA model in the Bethe lattice, when $c = 1$. The site and node contributions are given by:

$$\begin{aligned} e^{-\mu \phi_{site}} = Z_{site} &= \int e^{\mu(\sum^{K+1} \hat{a}(\underline{J}, \underline{h}) + |\sum^{K+1} \hat{u}(\underline{J}, \underline{h})|)} \prod_i^{c(K+1)} dP_i(h_i) \\ e^{-\mu \phi_{node}} = Z_{node} &= \int e^{\mu(\hat{a}(\underline{J}, \underline{h}) + |h_0 + \hat{u}(\underline{J}, \underline{h})|)} \prod_i^{c+1} dP_i(h_i) \end{aligned} \quad (15)$$

where Z_{site} and Z_{node} are partition functions that assure the normalization of the probability distributions at site and loop levels respectively.

Local distributions of fields $P(h)$ and messages $Q(u)$ hold the same relation than $\mathcal{P}(h)$ and $\mathcal{Q}(u)$ in equation (5), though they have different meanings. Using this relation and equation (13), the computation of $\phi(\mu)$ in (14) can be written in terms of $\mathcal{Q}[Q(u)]$ as:

$$-\mu \phi(\mu) = \frac{K+1}{c+1} \langle \log A[\underline{J}, \underline{Q}_a] \rangle - \frac{(Kc-1)}{c+1} \langle \log \int e^{\mu |\sum u_i|} \prod_i^{K+1} dQ_i(u_i) \rangle \quad (16)$$

where $\langle \cdot \rangle$ stands for the average over the order parameter distribution $\int \mathcal{Q}[Q]$ as well as over the quenched disorder distribution E_J . This is not, however, a variational expression for $\phi(\mu)$ and gives only valid results when the order parameter $\mathcal{Q}[Q]$ solves the self-consistent equation (11). The results obtained for the Replica Symmetric case can be recovered from the 1RSB expressions by taking the $\mu \rightarrow 0$ limit.

The complexity is related to the free energy $\phi(\mu)$ via a Legendre transform [11, 12]:

$$\Sigma(\mu) = \mu [\epsilon(\mu) - \phi(\mu)] \quad (17)$$

This justifies calling ϕ a free energy, and Σ and μ can be thought as the entropy and the temperature of a system whose configuration space is given only by the pure states of our original problem. On the other hand, given the relation of the complexity with the exponential abundance of states $\mathcal{N}(\epsilon) \sim \exp(N\Sigma(\epsilon))$, it is clear that the ground state of the system is one with zero complexity $\Sigma = 0$. This defines the point μ^* such that $\Sigma(\mu^*) = 0$ and $U_{1RSB} = \epsilon(\mu^*) = \phi(\mu^*)$ is the ground state prediction at the 1RSB approximation. Furthermore, given the usual Legendre relations

$$\epsilon(\mu) = \partial_\mu [\mu\phi(\mu)] \quad \Sigma(\mu) = \mu^2 \partial_\mu \phi(\mu) \quad (18)$$

it is clear that the point μ^* extremizes $\phi(\mu)$. Following the analogy with the replica method [1, 12], it can be shown that μ^* actually maximizes $\phi(\mu)$. As usual, it is sufficient to know $\phi(\mu)$ to obtain all other thermodynamic potentials, but let us mention that explicit expressions for $\epsilon(\mu)$ and $\Sigma(\mu)$ in terms of the order parameter can be derived straightforwardly [11, 12].

To finish the presentation of the 1RSB cavity method some words must be said about the numerical method used to solve the equation (11). Since $\mathcal{Q}[Q(u)]$ is a mathematical object very hard to deal with, this self-consistent equation is rarely solved analytically. The usual approach [11, 12, 16, 18, 28] is to represent the order parameter by a large population of distributions $Q(u)$, and to use a fixed-point method to solve eq. (11). In this work, each distribution $Q(u)$ is represented by the five numbers $p_{-2} \dots p_2$ (similar to (8)), and the order parameter consists of a population of $N \sim 10^4$ of such distributions. For each value of μ , the solution of the self-consistent equation is found by replacing several times ($\sim 10^2 N$) a randomly selected member of the distribution by the result of (12). After convergence, the free energy (16) is computed using other $\sim 5 * 10^3 N$ steps of the population dynamics algorithm.

B. RS-1RSB Stability Analysis

The stability under 1RSB perturbations of the RS solutions as a function of ρ can be studied with the method applied in [28, 29]. The replica symmetric self-consistent equation can be recovered from the 1RSB [28], by restricting the space of the 1RSB order parameter:

$$\mathcal{Q}[Q] \rightarrow \mathcal{Q}_{RS}[Q] = \sum_{q=-2}^2 p_q \delta^F(Q(u) - \delta_{u,q}) \quad (19)$$

In such a case, each distribution is forced to be deltaic and the re-weighting terms in (12) can be factorized out of the integrals. Then, all 1RSB expressions turn to be exactly the ones obtained at the RS level.

It is now fruitful to study the effect of the iteration procedure over a 1RSB parameter that is almost RS, except for a small perturbation of non-deltaic messages distributions:

$$\begin{aligned} \mathcal{Q}[Q] = & \sum_{q=-2}^2 p_q \delta^F(Q(u) - \delta_{u,q}) \\ & + \sum_{n=1}^{26} \int \pi_n(\{y\}) \delta^F(Q(u) - Q_n(\{y\})(u)) d\{y\} \end{aligned} \quad (20)$$

and to see how it evolves. The symbol $\{y\}$ stands for a subset of the parameters y_2, y_1, y_{-1}, y_{-2} (see equation below). Following [28, 29] this means that the order parameter has the following composition:

$$Q(u) = \begin{cases} \delta_{u,i} & \text{with probability } p_i, i \in (-2 \dots 2) \\ y_2 \delta_{u,2} + (1 - y_2) \delta_{u,1} & \text{with probability } \pi_1(y_2) \\ y_2 \delta_{u,2} + (1 - y_2) \delta_{u,0} & \text{with probability } \pi_2(y_2) \\ \vdots & \vdots \\ y_2 \delta_{u,2} + y_1 \delta_{u,1} + (1 - y_1 - y_2) \delta_{u,0} & \text{with probability } \pi_{11}(y_1, y_2) \\ \vdots & \vdots \\ y_2 \delta_{u,2} + y_1 \delta_{u,1} + \\ (1 - y_1 - y_2 - y_{-1} - y_{-2}) \delta_{u,0} + & \text{with probability } \pi_{26}(y_{-2}, y_{-1}, y_1, y_2) \\ y_{-1} \delta_{u,-1} + y_{-2} \delta_{u,-2} & \end{cases} \quad (21)$$

where the perturbation part is composed of all the 26 possible combinations of non-delta shaped distributions. We will refer to them as $Q_n(\{y\})(u)$ in general, and sometimes dropping the u for clarity. $Q_n(\{y\})(u)$ shall be interpreted as a function of u , where n and $(\{y\})$ are parameters, the former qualifying the type of non-deltaic distribution, and the latter defining the probabilities of each message in the distribution. Let us highlight that, while $Q_{26}(\{y\})(u)$ seems to contain all the other possibles $Q_n(\{y\})(u)$, it is not the case, since, to be meaningful in the context of the decomposition (21), all the components of the vector $\{y\}$ must be greater than zero. This is a way to focus our attention directly on the overall weight of each type of perturbation:

$$\Pi_n = \int \pi_n(\{y\})d\{y\} \quad (22)$$

For a first order study of the stability, the $\pi_n(\{y\})$ are supposed to be infinitesimal quantities such that, during the iteration, the presence of more than one non-delta shaped distributions in the cavity will be very improbable. The convolution of a given $Q_n(\{y\})$ with $cK - 1$ delta-shaped distributions in eq. (12) can yield, depending on the realization of the coupling constant, any of the distributions in (21). Considering all the possibilities and their probability of occurrence in eq. (12), we can construct the matrix $\mathbf{I}_{26 \times 26}$ of elements $i_{n,m}$ giving the probability that a non-delta-shaped distribution of type n turns into type m after the iteration. Then, after the iteration, the vector $\vec{\Pi} = (\Pi_1, \Pi_2, \dots, \Pi_{26})$ of the overall weight of the perturbations is transformed by

$$\vec{\Pi}' = \mathbf{I}\vec{\Pi} \quad (23)$$

A given RS solution is stable if all the eigen-values of \mathbf{I} are smaller than one:

$$\max \lambda(\mathbf{I}) < 1 \quad (24)$$

This is the general approach in studying the RS stability. In some cases, this approach may lead to simple and closed equations that allow analytical solutions, but in general, the properties of the matrix \mathbf{I} must be studied numerically.

III. RESULTS FOR THE TRIANGULAR HUSIMI LATTICE

In this section we apply the formalism described above to solve, at $T = 0$, the Edwards-Anderson model in the simplest of all Husimi lattices: the triangular lattice, with $c = 2, K = 1$ (see fig 1). Note that the case, $\rho = -1$ was recently extensively studied in [30] and is equivalent to the bi-coloring problem in an hyper-graph. Here we will keep $K = 1$ and concentrate our attention on the role of ρ in the thermodynamics of the system.

A. RS-solution

This graph allows closed expression for all the RS fixed points. For example, a careful analysis of (7) and (8) for this lattice leads to the definition of the following variables: $m_1 = p_1 - p_{-1}$, $s_1 = p_1 + p_{-1}$, $m_2 = p_2 - p_{-2}$ and $s_2 = p_2 + p_{-2}$, such that (7) may be written as:

$$\begin{aligned} m_1 &= (m_1 p_0 + \frac{s_1}{2}(m_1 + 2m_2))\rho - m_1(\frac{s_1}{2} + s_2 - p_0)\rho^2 \\ s_1 &= s_1(p_0 + s_2 + \frac{s_1}{4}) - m_1(m_2 - \frac{m_1}{4})\rho + \frac{m_1^2}{4}\rho^2 + (p_0 - \frac{s_1}{4})s_1\rho^3 \\ m_2 &= (s_1 m_1 + s_2 m_1 - s_1 m_2 + 2m_2)\frac{\rho}{2} + (m_1 s_1 + s_2 m_1 + s_1 m_2 + 2p_0 m_2)\frac{\rho^2}{2} \\ 2p_0 &= s_1^2 + s_2^2 + s_1 s_2 + 2p_0 + m_1 m_2 \rho - (m_1^2 + m_2^2 + m_1 m_2)\rho^2 - (2p_0(1 - p_0) + s_1 s_2)\rho^3 \\ s_2 &= 1 - p_0 - s_1 \end{aligned} \quad (25)$$

It is easy to check that, independently of ρ , a trivial paramagnetic solution (P) where only $u = 0$ messages have a non-zero probability $p_0 = 1$, always exists:

$$\mathcal{Q}_P(u) = \delta_{u,0} \quad (26)$$

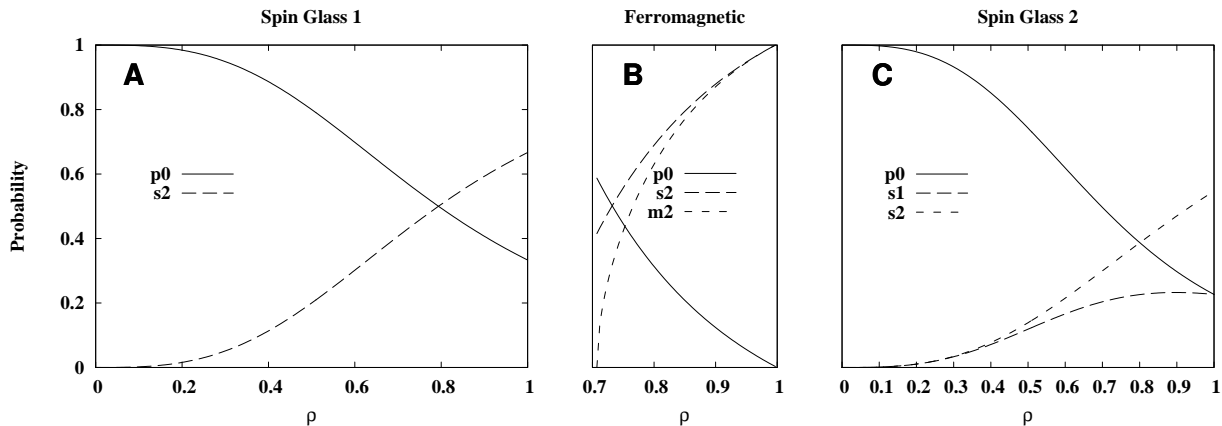


FIG. 2: The solution of the RS equations for the triangular Husimi lattice ($c = 2$ and $K = 1$). Panel **A** is the first spin-glass solution (SG-1). Panel **B** represents the ferromagnetic solution. In panel **C** appears the second spin-glass solution (SG-2). The variables are defined in section III A.

On the other hand, setting the values of m_1 and s_1 to zero, i.e. $p_1 = p_{-1} = 0$, automatically satisfies the first two equations in (25). With the three remaining equations, we can find three solutions. The first one is a spin glass paramagnetic solution (SG-1) with $p_0 = (2\rho^3 + 1)^{-1}$, $m_2 = 0$, $s_2 = 1 - p_0$:

$$\mathcal{Q}_{SG-1}(u) = \frac{\rho^3}{2\rho^3 + 1} \delta_{u,-2} + \frac{1}{2\rho^3 + 1} \delta_{u,0} + \frac{\rho^3}{2\rho^3 + 1} \delta_{u,2} \quad (27)$$

that is valid for $\rho \geq \rho_{SG-1} = 0$ and is shown in panel **A** of figure 2. The second and third solutions are actually the same 2-degenerated ferromagnetic solution with $p_0 = \frac{1-\rho}{\rho^2}$, $s_2 = 1 - p_0$ and $m_2^2 = (\rho^2 + \rho - 1)^2 \rho^{-6} - 2(\rho^2 + \rho - 1)(1 - \rho)\rho^{-3}$:

$$\mathcal{Q}_F(u) = \frac{s_2 - m_2}{2} \delta_{u,-2} + \frac{1 - \rho}{\rho^2} \delta_{u,0} + \frac{s_2 + m_2}{2} \delta_{u,2} \quad (28)$$

valid for $\rho \geq \rho_F = \frac{1}{\sqrt{2}} \simeq 0.7071$. The dependencies of p_0 , s_2 and m_2 with ρ appear in panel **B** of figure 2.

There is yet another spin glass paramagnetic solution with $s_1 \neq 0$, $m_1 = 0$ and $m_2 = 0$ that we will call SG-2. It differs from the SG-1 in that $p_1 = p_{-1} > 0$. The dependencies of s_1 , s_2 and p_0 for this solution are shown in the panel **C** of figure 2. Like the other solutions described above, this solution can be analytical expressed as a function of ρ . However, the resulting algebraic expression is quite large and does not add clarity to the remaining discussion, so we do not write it explicitly here. Just note (figure 2) that this solution exists only for $\rho \geq \rho_{SG-2} = 0$. At this point it is worth mentioning that the notations SG-1 and SG-2 refer to the non-trivial structure (although symmetric) of the distributions, but one must keep in mind that the solution is ergodic and does not represent a true glassy system.

Each of the four solutions described above defines an energy function $U(\rho)$ by eq. 9) (see figure 3). Except for the second spin glass paramagnetic solution, which we leave to the interested reader to work out, the expressions for the energy are rather simple:

$$\begin{aligned} U_P &= -\frac{2}{3}(2 + \rho^3) \\ U_{SG-1} &= -\frac{2}{3} \frac{2 + 9\rho^3 + 12\rho^6}{(1 + 2\rho^3)^2} \\ U_F &= -\frac{2}{3} \frac{(-1 + 3\rho - 7\rho^3 + 6\rho^4 - \rho^6 + 3\rho^7)}{3\rho^6} \end{aligned} \quad (29)$$

Summarizing, the RS calculations show that: *i*) a trivial paramagnetic solution exists for all ρ ; *ii*) at $\rho = \rho_{SG-1} = \rho_{SG-2} = 0$ two spin glass paramagnetic solutions appear and are valid up to $\rho = 1$; *iii*) for $\rho > \rho_F = 2^{-1/2}$ one also finds a ferromagnetic solution. Note that, in the scale of the figure 3, it is hard to differentiate the actual energies of the different solutions for a wide range of values of ρ . As we demonstrate in the next section, the same is true when compared with the 1RSB solution. However, we will show that for other lattices the situation is different.

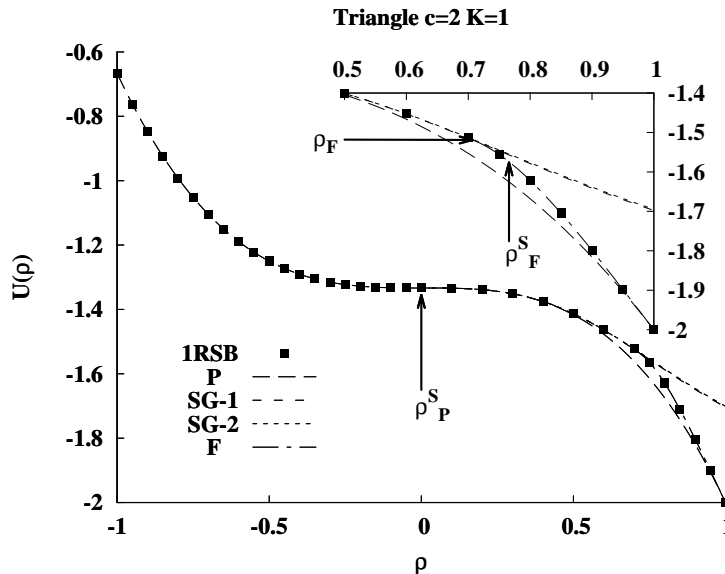


FIG. 3: Energies for the different RS solutions and the 1RSB approximation $\phi(\mu^*)$ as a function of ρ for the triangular Husimi lattice ($c = 2$, $K = 1$). We represent also the stability threshold $\rho_P^S = 0$ of the trivial paramagnetic solution. The caption shows the point in which the ferromagnetic solution appears ρ_F , and the point where it becomes stable ρ_F^S .

B. Stability analysis of the RS solutions

Though the general method given in the introduction is always valid, we will try to keep the stability analysis as simple as possible. The trivial paramagnetic solution can be studied, for instance, with only one general perturbation $Q_{26}(y_{-2}, y_{-1}, y_1, y_2) = y_{-2}\delta_{u,-2} + y_{-1}\delta_{u,-1} + (1 - y_{-2} - y_{-1} - y_1 - y_2)\delta_{u,0} + y_1\delta_{u,1} + y_2\delta_{u,2}$

$$\begin{aligned} \mathcal{Q}[Q] &= \delta^F(Q(u) - \delta(u, 0)) \\ &+ \int \pi(y_2, y_1, y_{-1}, y_{-2}) \delta^F(Q(u) - Q_{26}(y_2, y_1, y_{-1}, y_{-2})) dy_2 dy_1 \dots \end{aligned} \quad (30)$$

The idea is to follow the overall weight of the perturbation $\Pi = \int \pi(y_2, y_1, y_{-1}, y_{-2}) dy_2 dy_1 dy_{-1} dy_{-2}$ for the iteration (12). The reason behind the success of such a simple analysis lies in the fact that the iteration eq. (12) has a very naive behavior when we consider the convolution of the paramagnetic solution with a perturbation. Depending on the realization of the coupling constants $J_{i,j}$, the convolution of the perturbation $Q_{26}(y_{-2}, y_{-1}, y_1, y_2)$ and the RS solution $\delta(u, 0)$ can only produce one of the following three results:

$$\begin{aligned} \delta_{u,0} * Q_{26}(y_{-2}, y_{-1}, y_1, y_2) &\rightarrow \delta_{u,0} \\ \delta_{u,0} * Q_{26}(y_{-2}, y_{-1}, y_1, y_2) &\rightarrow Q_{26}(y_2, y_1, y_{-1}, y_{-2}) \\ \delta_{u,0} * Q_{26}(y_{-2}, y_{-1}, y_1, y_2) &\rightarrow Q_{26}(y_{-2}, y_{-1}, y_1, y_2) \end{aligned}$$

where we are using the symbol $*$ to represent the right-hand side of eq. (12). Averaging over all possible couplings, we found that the last two situations take place with a probability $\frac{1+\rho^3}{2}$. Then, also taking into account a combinatorial factor of 2, the overall weight of the perturbation evolves following:

$$\Pi'_P = (1 + \rho^3)\Pi_P \quad (31)$$

showing that for all $-1 \leq \rho < \rho_P^S = 0$ the paramagnetic solution $Q_P(u) = \delta_{u,0}$ is stable, while it is unstable for $\rho > 0$. To determine the stability of the solution at $\rho_P^S = 0$ one must use a second order perturbation.

Unfortunately, in general, such a simple analysis is not applicable. For instance, the spin glass paramagnetic solution, SG-1, when convolved with Q_{26} , can yield mixed distributions of other types. Then, in order to keep analytical expressions, we consider in this case two other types of perturbations:

$$\begin{aligned} Q_n(y) &= (1-y)\delta_{u,0} + y\delta_{u,2} \\ Q_m(y) &= y\delta_{u,-2} + (1-y)\delta_{u,0} \end{aligned} \quad (32)$$

Both the spin glass paramagnetic solution, SG-1, and the ferromagnetic solution, F, have only messages $u \in \{-2, 0, 2\}$. Then, the convolution with the perturbations $Q_{n,m}$ produces one of the following results:

$$\begin{aligned} Q_{SG-1,F} * Q_{n,m}(y) &\rightarrow \delta_{u,0} \\ Q_{SG-1,F} * Q_{n,m}(y) &\rightarrow \delta_{u,2} \\ Q_{SG-1,F} * Q_{n,m}(y) &\rightarrow \delta_{u,-2} \\ Q_{SG-1,F} * Q_{n,m}(y) &\rightarrow Q_m(y') \\ Q_{SG-1,F} * Q_{n,m}(y) &\rightarrow Q_n(y') \end{aligned}$$

where only the last two situations are responsible for the evolution of the perturbation. This set of perturbations is closed under the iteration equation (12) and therefore suitable for analytical treatment.

For the spin glass solution, SG-1, the matrix for the evolution of the perturbation $\mathbf{I}_{2 \times 2}^{SG-1}$ is symmetric, with elements:

$$\begin{aligned} i_{n,n} = i_{m,m} &= \frac{1 + 3\rho^3 + \rho + \rho^2 - 2\rho^5}{2(1 + 2\rho^2)} \\ i_{n,m} = i_{m,n} &= \frac{1 + 3\rho^3 - (\rho + \rho^2 - 2\rho^5)}{2(1 + 2\rho^2)} \end{aligned}$$

The largest of its eigenvalues is $\lambda = \frac{1+3\rho^3}{1+2\rho^3}$ which is always greater than one, for $\rho > 0$. This means that the spin glass SG-1 solution is always unstable.

For the ferromagnetic solution, the matrix $\mathbf{I}_{2 \times 2}^F$ has the following structure

$$\begin{aligned} i_{n,n} = i_{m,m} &= \frac{1}{2} \left(1 + \frac{1}{\rho} - \rho - 2\rho^2 \right) \\ i_{n,m}^+, i_{m,n}^- &= \frac{3\rho^2 - 1}{2\rho} \pm \frac{1}{\rho^2} \sqrt{(\rho^4 - (\rho - 1)^2)(2\rho^2 - 1)} \end{aligned}$$

where the terms $i_{n,m}^+, i_{m,n}^-$ differ in the sign in front of the square root. The limiting condition for the stability $\max \lambda(\mathbf{I}) = 1$ turns out to be equivalent to the solution of $\rho^6 + \rho^4 - 2\rho^3 + \rho^2 + \rho - 1 = 0$. This defines the point $\rho_F^S \simeq 0.765942$ where the ferromagnetic solution becomes stable.

For the spin glass paramagnetic solution SG-2 it was impossible to find a closed subset of perturbations smaller than the full set. Therefore we studied its stability using the full matrix $\mathbf{I}_{26 \times 26}$. Given the size of the matrix, and the non-simple dependence of this solution with ρ , the study of the stability was done numerically. We calculated all the 26 eigenvalues of $\mathbf{I}_{26 \times 26}$ and found that some of them were always above 1 in the interval $0 < \rho < 1$. This means that the spin glass solution (SG-2), like the (SG-1), is always unstable.

Note, that the results obtained for the SG-1 and ferromagnetic solutions where only a subset of perturbations were studied, can be considered only as lower-bound approximations for the stability. For the SG-1 the full 26 perturbations procedure can be done analytically, and it appears that the highest eigenvalue was, in fact, the one we found with the restricted perturbation method. For the ferromagnetic solution it is harder to get an analytic expression for the eigenvalues of the full matrix $\mathbf{I}_{26 \times 26}$, but yet we checked numerically that all the eigenvalues of this matrix were indeed equal or smaller than the one found within the restricted perturbation analysis. In summary, the triangular Husimi lattice with $K = 1$ has a stable RS trivial paramagnetic solution for $-1 \leq \rho < \rho_P^S = 0$, has a stable ferromagnetic solution $Q_F(u)$ when $\rho_F^S \leq \rho < 1$, and two spin glass paramagnetic solutions that are unstable to replica symmetry breaking. These points of stability are shown in figure 3.

C. 1RSB solution

The 1RSB approximation for the free energy of a model is a formalism more general than the Replica Symmetric calculation. Thus, in the calculation of the free energy, we do not need to restrict ourselves to the interval $\rho_P^S < \rho < \rho_F^S$

where the RS solutions are unstable. Instead we can do the 1RSB calculation in the whole interval $-1 \leq \rho \leq 1$, and the RS solutions will still be found if they are thermodynamically significant, which is a stronger condition than stability.

Using the population dynamics described in section II A 2 we computed $\phi(\mu)$ for different μ . In figure 3 we compare the ground-state predictions U_{RS} and U_{1RSB} for both approximations (RS and 1RSB) as a function of ρ . In the caption we show how the 1RSB solution collapses into the F solution for $\rho > \rho_F^S$. Unfortunately, with the resolution of figure 3 it is impossible to differentiate the ground state energy in the 1RSB approximation from the energy of the RS solutions within the region in which no RS solution is stable, although the order parameter $\mathcal{Q}[Q]$ showed to be non-trivial, i.e. not having the form of (19).

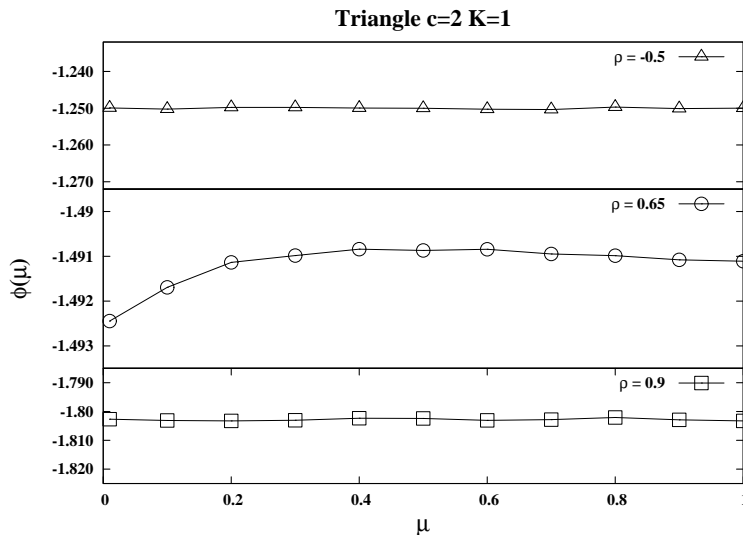


FIG. 4: Free energy $\phi(\mu)$ of the 1RSB solution for the triangular Husimi lattice ($c = 2$, $K = 1$) for different values of ρ . Top panel: paramagnetic region, Middle: 1RSB region and Bottom: ferromagnetic. The flat curves are representative of RS solutions, while the curve in the 1RSB region has a clear non trivial maximum $\phi(\mu^*) = U_{1RSB}$ at $\mu \simeq 0.6$.

For the sake of understanding the qualitative differences between the RS and the 1RSB solution, we show the curve $\phi(\mu)$ for three different ρ in figure 4. The lower curve corresponds to the ferromagnetic region ($\rho > \frac{1}{\sqrt{2}}$), the upper to the paramagnetic (P) interval, and the middle curve to the 1RSB zone. In the paramagnetic and ferromagnetic regions, $\phi(\mu)$ is flat, as expected. It has zero derivative and hence zero complexity, meaning that the solution space is not clustered and that the RS assumptions are valid. Furthermore, a detailed analysis of the order parameter shows that it actually has the RS structure (19). On the other hand, in the 1RSB region ($\rho = 0.65$) $\phi(\mu)$ is convex and has a maximum at $\mu = \mu^* \simeq 0.6$, and the order parameter is genuine 1RSB (not made of deltaic distributions) for all values of μ . The highest point of this curve defines the 1RSB approximation for the ground state energy $U_{1RSB} = \phi(\mu^*)$.

The learned reader will find rare that a highly-frustrated system, as the Husimi triangular lattice with an excess of antiferromagnetic interactions ($\rho < 0$), does not have a 1RSB solution. He might argue that the proved stability of the trivial paramagnetic RS solution is not enough to rule out other solutions. In fact, the absence of 1RSB solution may well be an artifact due to the random initial conditions used in the population dynamics. Fortunately, with the same tools used to analyze the stability of RS solutions, it is possible to prove (see appendix A) that any $\mathcal{Q}[Q(u)]$ solution of the self-consistent equation (11) is unstable to a paramagnetic perturbation $\mathcal{Q}[Q] = \pi \delta^F(Q(u) - \delta_{u,0})$. This rules out any possible stable solution except for the complete paramagnetic one $\mathcal{Q}_P[Q(u)] = \delta^F(Q(u) - \delta_{u,0})$, rendering the trivial paramagnetic solution the only thermodynamically relevant in the region $-1 \leq \rho < 0$. It must be kept in mind, however, that at finite temperature a 1RSB solution with real-valued fields, which are not embedded in our parameterization, may facilitate a RS-1RSB transition in this zone.

To help the intuition, let us look closer to the case $\rho = -1$. In this case, each triangle has a minimum energy 6-times degenerated, and only 2 excited states. It is true that in all the states of minimum energies, one of the bonds of the triangle is violated, but one cannot forget that this is anyway the ground state of the triangle. Then, because this state is highly-degenerated, it is not hard to imagine that there is a lot of freedom, even on the large scale of the network, to have all the triangles "satisfied". Of course, this argument is valid provided K is low. If K is high enough, each spin will be connected to a large number of triangles, and therefore, the freedom of choice will be reduced and

eventually may disappear. This, in fact, should turn the problem to the non-trivial 1RSB scenario predicted in[30] for $K > 6$.

IV. GENERAL HUSIMI LATTICES

The procedure described in the introduction, and applied to the study of the triangular Husimi graph, is also applicable to all other Husimi graphs. The main difference arises in the difficulty in generalizing the analytical results obtained above. For instance, the equation (7) is still parameterized by $p_{-2}, p_{-1}, p_0, p_1, p_2$, but since each term has degree $c \cdot K$ on these probabilities, it is very hard to write closed equations in terms of ρ . The absence of closed expressions for these probabilities also makes it impossible to express the RS-1RSB instability analytically. However we can always solve numerically the set of five equations (7) on the probabilities p_i for each value of ρ , and check numerically the eigenvalues of the stability matrix for such solutions. The only exception that allows a full analytical treatment independently of K and c , is the trivial paramagnetic solution $Q_P = \delta_{u,0}$, that is obviously a solution of equation (7) for all the Husimi lattices.

A. The trivial paramagnetic solution

The result obtained for the trivial paramagnetic solution in the cactus can be easily generalized to all kinds of pure and regular Husimi lattices, with generic loop size $c + 1$ and degree $K + 1$. The paramagnetic solution is always valid, but it changes from one type of graph to another. To study the transition RS-1RSB we consider again a perturbed order parameter of type (30). In the general case equation (12) is a convolution of $c \cdot K$ distributions. Again, the convolution of paramagnetic distributions reproduces a paramagnetic distribution:

$$(\delta_{0,u*})^{cK} \rightarrow \delta_{0,u}$$

The non-trivial case is the convolution with the perturbed distributions Q_{26} that are present in the order parameter $\mathcal{Q}[Q]$ in an amount proportional to $\pi_{26}(y_2, y_1, y_{-1}, y_{-2})$ (see equation (30)). Depending on the realization of the coupling constants, the integration of eq. (12) may have three different results:

$$\begin{aligned} (\delta_{u,0*})^{cK-1} Q_{26}(y_2, y_1, y_{-1}, y_{-2}) &\rightarrow \delta_{u,0} \\ (\delta_{u,0*})^{cK-1} Q_{26}(y_2, y_1, y_{-1}, y_{-2}) &\rightarrow Q_{26}(y_2, y_1, y_{-1}, y_{-2}) \\ (\delta_{u,0*})^{cK-1} Q_{26}(y_2, y_1, y_{-1}, y_{-2}) &\rightarrow Q_{26}(y_{-2}, y_{-1}, y_1, y_2) \end{aligned} \quad (33)$$

It is easy to check that, independently of the loop size $c + 1$ and the connectivity $K + 1$ of the Husimi graph, the last two outcomes (those that are responsible for the propagation of the perturbation) take place only when an even number of couplings $J_{i,j}$ are anti-ferromagnetic. The probability to have an even number of anti-ferromagnetic couplings around a loop can be computed as:

$$\sum_{q=0}^{(c+1)/2} \left(\frac{1+\rho}{2}\right)^{c+1-2q} \left(\frac{1-\rho}{2}\right)^{2q} \binom{2q}{c+1} = \frac{1}{2}(1 + \rho^{c+1}) \quad (34)$$

The upper limit of the sum is taken to be the higher integer value not greater than $(c+1)/2$. Since the perturbation Q_{26} can occur in any of the $c \cdot K$ cavity biases distribution of eq. (12), one needs to consider a cK combinatorial factor in the previous expression. Thus we get that the perturbation weight $\Pi_P = \int \pi(y_2, y_1, y_{-1}, y_{-2})$ evolves through:

$$\Pi_P = \frac{cK}{2}(1 + \rho^{c+1})\Pi_P \quad (35)$$

The condition of stability is the damping of the perturbation $\frac{cK}{2}(1 + \rho^{c+1}) < 1$ which has no solution for odd c , i.e. for even loop sizes as squares, hexagons, etc. The general solution:

$$\rho < \rho_P^S = - \left(\frac{cK - 2}{cK}\right)^{\frac{1}{c+1}} \quad (36)$$

is valid for odd loop sizes like the triangle, the pentagon, etc. For values of $\rho < \rho_P^S$ the paramagnetic solution $\mathcal{Q}(u) = \delta_{0,u}$ is stable. On the other hand, for even loop sizes the paramagnetic solution is never stable.

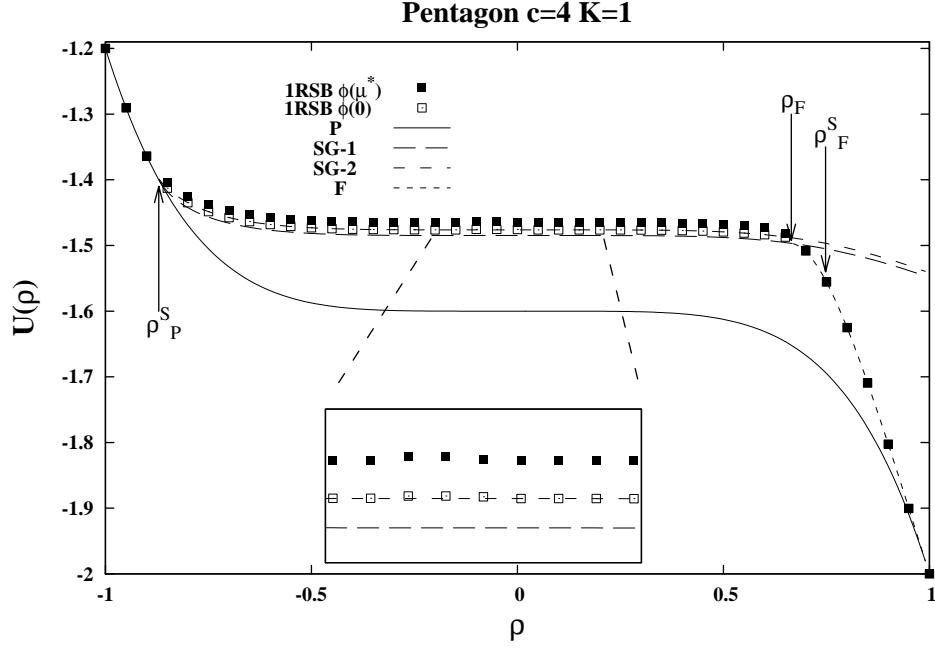


FIG. 6: Energies for the different RS solutions and the 1RSB solution as a function of ρ for pentagonal Husimi lattice ($c = 4$, $K = 1$). The stability threshold for the P and F solutions are signaled. The caption shows difference between the 1RSB approximation $U_{1RSB} = \phi(\mu^*)$ (black squares) and the energy of the RS solutions. White squares represent $\phi(0)$ and coincide with the energy of the SG-2 solution.

solutions are always unstable to 1RSB perturbations, and the ferromagnetic solution has a non-trivial stability point ρ_F^S above which it becomes stable (see figures 5 and 6). In table (I) we present, for different c and K , the numerical values for these stability points and for the appearance of the ferromagnetic solution ρ_F .

Husimi	ρ_P^S	ρ_F	ρ_F^S
$c = 2, K = 1$	0	$1/\sqrt{2} \simeq 0.707$	0.766
$c = 3, K = 1$	—	0.671	0.749
$c = 4, K = 1$	$-\sqrt[5]{\frac{1}{2}} \simeq -0.8706$	0.665	0.748
$c = 2, K = 2$	$-\sqrt[3]{\frac{1}{2}} \simeq -0.7937$	0.534	0.631

TABLE I: The paramagnetic and ferromagnetic solutions are stable to the left and right of ρ_P^S and ρ_F^S respectively. The stability of the paramagnetic solution is found analytically (see section IIB). The point in which the ferromagnetic solutions first appears within the RS approximation ρ_F , as well as the stability of this solution, are found numerically by solving the RS self consistent equation (7) for different ρ .

The picture that emerges from these calculations is the following: above ρ_F^S , the ferromagnetic RS solution is stable to 1RSB perturbations and thermodynamically relevant. Below this point, both spin-glass solutions are unstable. On the other hand, the stability of the trivial paramagnetic solutions (P) depends on the parity of the loops. In Husimi lattices with even loop sizes ($c+1 = 4, c+1 = 6$, etc) this phase is never stable, while in lattices with odd loops sizes, this phase becomes stable below ρ_P^S .

C. 1RSB Solutions

For each Husimi lattice and for each value of ρ , the 1RSB free energy $\phi(\mu)$ is computed using the usual method of population dynamics. The 1RSB prediction for the energy of the model is given by $U_{1RSB} = \phi(\mu^*)$ where μ^* maximizes ϕ . On the other hand, the limit $\mu \rightarrow 0$ must recover the RS equations and $\phi(0)$ must coincide with one of the replica symmetric solutions.

In figures 5 and 6, $U_{1RSB} = \phi(\mu^*)$ and $\phi(0)$ are shown simultaneously for the square and pentagon Husimi lattices with $K = 1$. In both types of graphs, the ferromagnetic solution is thermodynamically relevant for large ρ , as our intuition tells us. In the case of odd loop sizes, the situation is similar to the one found in the triangular Husimi lattice: the trivial paramagnetic solution seems to be the thermodynamically relevant for negative enough ρ .

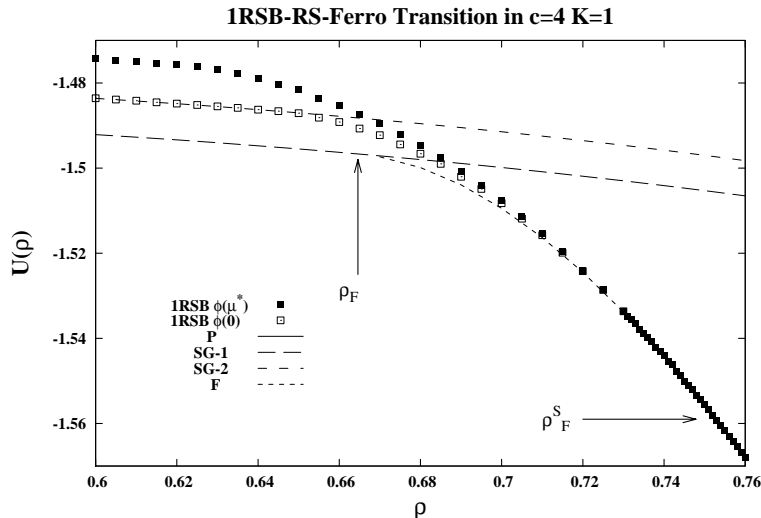


FIG. 7: Energy versus ρ close to the *1RSB-Ferromagnetic* transition. The real thermodynamic behavior of the system is defined by the black squares. The replica symmetric ferromagnetic phase is not only stable above ρ_F^S , but also thermodynamically relevant, as the 1RSB solution smoothly becomes RS (see eq. 19) as $\rho \rightarrow \rho_F^S$.

Summarizing, below the ferromagnetic stable region $\rho_F^S < \rho \leq 1$, the model has always a thermodynamically relevant 1RSB solution. In Husimi lattices with even loop sizes ($c+1 = 4$, $c+1 = 6$, etc.) this phase goes till $\rho = -1$, while in Husimi graphs with odd loop sizes and depending on K , this 1RSB phase may disappear for negative enough ρ and in this case, the thermodynamics of the system is controlled by a trivial paramagnetic solution. However, it is worth mentioning that for large cK , $\rho_P^S \rightarrow -1$. Moreover, we will show below that the 1RSB solution may extend below ρ_P^S , so, in more general cases, we expect that this solution becomes thermodynamically relevant also for $\rho = -1$ [30].

To understand the characteristics of the transitions between the RS to the 1RSB phases we take the $c = 4, K = 1$ case as a model. We made a close-up and a careful calculation around the *1RSB-Ferromagnetic* and the *1RSB-Paramagnetic* transitions. They appear in figures 7 and 8, respectively. In both cases the simulations were done adiabatically, starting from the 1RSB zone and slowly varying ρ towards the transition points and working always at μ^* . In this way we guarantee that the algorithm finds (if it exists) the 1RSB solution.

As the figure 7 suggests, the *1RSB-Ferromagnetic* transition is continuous. Increasing ρ , a close inspection of the structure of the order parameter $\mathcal{Q}[Q(u)]$ (represented by the population of distributions $Q(u)$) shows that the amount of deltaic distributions $Q(u) = \delta_{u,u_0}$ grows smoothly as ρ approaches ρ_F^S .

On the other hand (see figure 8), the *1RSB-Paramagnetic* transition is quite different. There is region $\rho_{1RSB} < \rho < \rho_P^S$ in which the thermodynamically relevant solution is 1RSB, but where the RS solution is stable under 1RSB perturbations. Then, below the point $\rho_{1RSB} \sim -0.89$ the paramagnetic solution has higher energy and becomes thermodynamically relevant. Note on the inset that below this point there is still a region where the algorithm finds a non-trivial 1RSB solution of lower energy. This suggests that in this zone 1RSB solutions may appear but are exponentially rare. Then, by further decreasing ρ , the population dynamics finds only the trivial paramagnetic solution. The inspection of the distribution shows that this transition is discontinuous. Above ρ_{1RSB} the order parameter $\mathcal{Q}_{1RSB}[Q(u)]$ is free of deltaic distributions $Q(u) = \delta_{u,u_0}$ and below ρ_{1RSB} the solution is completely paramagnetic.

D. The limit of the Bethe lattice

Finally, we focused on the unbiased model $\rho = 0$. In this case, all the Husimi lattices, with the exception of the triangular ($c = 2$ and $K = 1$), are at least 1RSB (see eq. (36)).

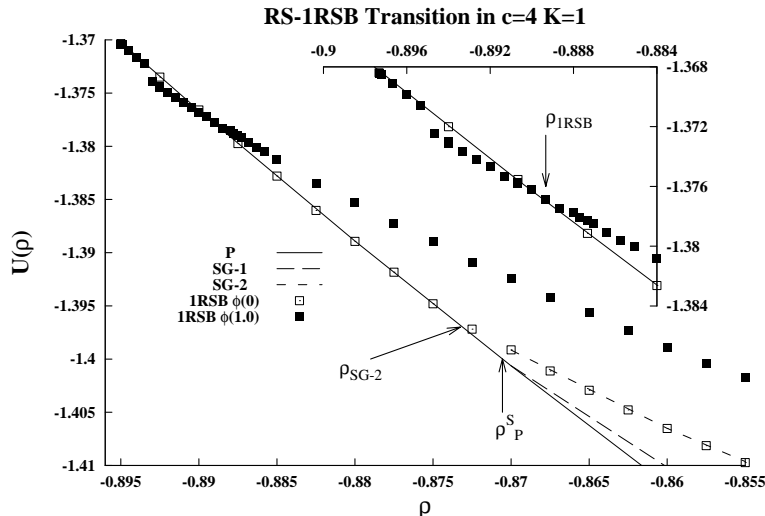


FIG. 8: Energy versus ρ close to the *1RSB-Paramagnetic* transition. The real thermodynamic behavior of the system is defined by the black squares, except for the unstable region in which the adiabatic continuation of the 1RSB solution goes below the paramagnetic curve (see caption). For $\rho < \rho_{1RSB}$ the thermodynamically relevant order parameter is the RS trivial paramagnetic solution. The transition *1RSB-Paramagnetic* is not continuous: the structure of the order parameter changes abruptly when crossing ρ_{1RSB} .

If we refer to the Husimi lattice considering only the local connectivity of the sites (number of neighbors), then, a Husimi lattice with degree $K + 1$ is locally very similar to a Bethe lattice with degree $k + 1 = 2(K + 1)$. In table II we present a few ground state energies at the 1RSB level of approximation for different Husimi lattices and compare them with similar results for Bethe lattices. Note that for $c = 7, K = 1$ and $c = 5, K = 2$, the differences between the Bethe and the Husimi ground states are already very small.

Husimi	U_{GS}
$c = 2, K = 1$	$-\frac{4}{3} = -1.333$
$c = 3, K = 1$	-1.444 ± 0.002
$c = 5, K = 1$	-1.468 ± 0.002
$c = 7, K = 1$	-1.470 ± 0.002
Bethe, $k = 3, c = \infty, K = 1$	-1.471 ± 0.002

Husimi	U_{GS}
$c = 2, K = 2$	-1.471 ± 0.002
$c = 3, K = 2$	-1.819 ± 0.002
$c = 5, K = 2$	-1.823 ± 0.002
Bethe, $k = 5, c = \infty, K = 2$	-1.825 ± 0.002

TABLE II: Ground state energies within the 1RSB approximation of different Husimi lattices for $\rho = 0$.

This similarity goes beyond the ground state calculations. In figure 9 we plot the free energy $\phi(\mu)$, and the complexity $\Sigma(\epsilon)$ for different Husimi lattices with $K = 2$ and $\rho = 0$ and for the Bethe lattice. As expected, the figure shows a clear maximum at $\phi(\mu^*)$ and the two usual branches in the $\Sigma(\epsilon)$ plot[12]. From these plots, we may also conclude that the local similarity between Bethe and Husimi lattices, for which the relation $k + 1 = 2(K + 1)$ holds, turns out to be true, on thermodynamic grounds for loop sizes greater than $c + 1 = 6$ ($c + 1 = 8$ if $K = 1$). This suggest that, at least for the EA model, the Bethe approximation may work even under conditions less restrictive than loop sizes of order $\ln N$.

V. CONCLUSIONS

We solved the Edwards-Anderson model in a Husimi graph at $T = 0$. We presented closed analytical (RS) expressions as a function of ρ for the existence and the stability of a trivial paramagnetic solution (P). For the triangular Husimi lattice ($c = 2$ and $K = 1$) we obtained similar expressions for the appearance and the stability of two spin-glass solutions (SG-1, SG-2) and a ferromagnetic solution (F). For other cases, these points were calculated numerically (see table I). Within the 1RSB approximation we obtained, using a population dynamics algorithm, the value of the ground state energies of different lattices as a function of ρ (see figures 5 and 6).

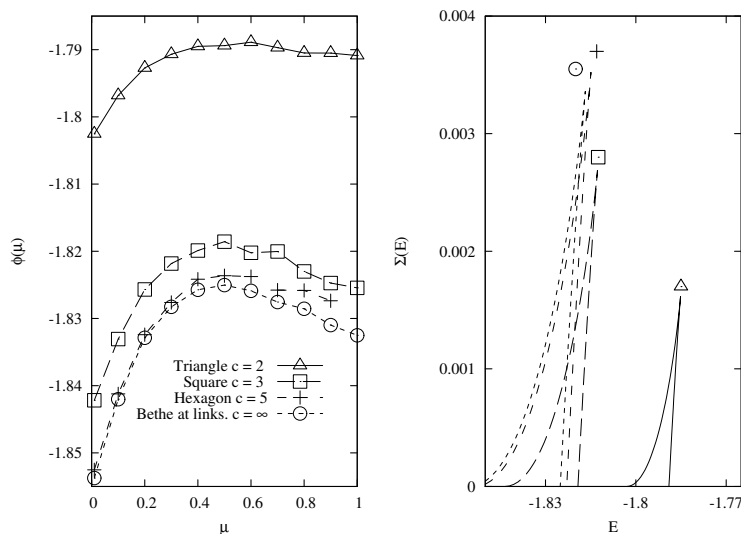


FIG. 9: Free energy $\phi(\mu)$ (left) and complexity $\Sigma(\epsilon)$ (right) of different Husimi lattices at $\rho = 0$ and $K = 2$. The graphics for $K = 1$ are similar. Also represented the EA solution in the Bethe lattice with degree $k = 5$. The symbols in the right panel correspond to the legend in the left panel. The early coincidence ($c = 5$) between our short loop model in Husimi graphs, and the short-loop-free model in the Bethe lattices, gives a thermodynamic threshold for the relevance of loops.

The main picture emerging from this work is that for Husimi lattices with even loop sizes, the system is at least 1RSB in all the range $-1 < \rho < \rho_F^S(c, K)$. Above $\rho_F^S(c, K)$ the model has a RS ferromagnetic solution, and the transition from the 1RSB phase to the ferromagnetic one is continuous. On the other hand, for lattices with odd loop sizes a trivial paramagnetic solution is stable under 1RSB perturbations up to $\rho_P^S = -\left(\frac{cK-2}{cK}\right)^{\frac{1}{c+1}}$, in addition for small K this solution may become thermodynamically relevant below $\rho_{1RSB} \leq \rho_P^S$ where the order parameter jumps discontinuously from a non-trivial 1RSB solution towards trivial paramagnetic distributions. For the particular case of the triangular lattice with $K = 1$ it was proven that the trivial paramagnetic solution is actually the unique and thermodynamically relevant solution (at least in the 1RSB frame) for all $\rho < 0$.

Finally, we focused on the $\rho = 0$ case and computed the ground state energies for different values of c and K (see table II). Our results suggest that the energy and complexity of the EA model in Husimi lattices with loop sizes $c + 1 \geq 8$ are already well described by an equivalent short-loop-free EA model in a Bethe lattice. This, in turn, can be considered a thermodynamic threshold for the *shortness* of loops, less restrictive than the usual $\sim \log(N)$.

VI. ACKNOWLEDGMENTS

We thank F. Ricci-Tersenghi and M. Pretti for useful discussions and comments. We also acknowledge the support of the NET-61 from the ICTP, and the ICTP for kind hospitality.

VII. APPENDIX A

Let us prove that the trivial paramagnetic solution is actually the only thermodynamically relevant solution of the self-consistent equation (11) for the triangular Husimi lattice ($c = 2$ and $K = 1$), in the interval $(-1 \leq \rho < \rho_P^S = 0)$. In doing so, we will follow exactly the same procedure used to study the instability of the Replica Symmetric solutions. We will presume that a non-trivial solution exists for the self-consistent equation, and we will show that it is unstable to small variations of the probability of paramagnetic distributions of messages $Q(u) = \delta_{u,0}$.

Let us call $\mathcal{Q}[Q]$ the solution of the self-consistent equation at 1RSB level of approximation. A perturbed order parameter would be $\mathcal{Q}[Q] + \pi \delta^F(Q(u) - \delta_{u,0})$. If we write down the self-consistent equation (11) using this order parameter, and keep to the first order in π in the right-hand side, we will get the following equation for the evolution

of the perturbation weight:

$$\pi' \delta_{u,0} = 2\pi E_J \int \delta^{(F)}(Q - \hat{Q}[J_{0,1}, J_{1,2}, J_{2,0}, Q, \delta_{u,0}]) dQ[Q] \quad (38)$$

where E_J is the expectation over the coupling constants J , and the 2 multiplying the integral is a combinatorial factor. The possible realizations of the disorder can be grouped into two sets: those with an odd number of antiferromagnetic interactions, like $(-1, -1, -1)$ and $(-1, 1, 1)$; and those with an even number like $(1, 1, 1)$ and $(-1, -1, 1)$. Elements of the first group occur with a probability

$$P_{\text{frustration}} = \left(\frac{1+\rho}{2}\right)^3 + 3\left(\frac{1+\rho}{2}\right)^2\left(\frac{1-\rho}{2}\right) = \frac{1-\rho^3}{2} \quad (39)$$

while the other group has a complementary probability. Whenever the disorder happens to be frustrated (first group), the convolution $\hat{Q}[\underline{J}, Q, \delta_{u,0}] = \delta_{u,0}$ regardless of the actual distribution Q . On the other hand, if the disorder around the triangle is not frustrated (second group) $\hat{Q}[\underline{J}, Q, \delta_{u,0}] = Q(u)$, thus reproducing the probability distribution of $Q[Q(u)]$. Then the contribution to the perturbation is only given by the frustrated triangles, and we get for the iteration:

$$\pi' = 2\pi P_{\text{frustración}} \quad (40)$$

The instability condition would be given by:

$$2P_{\text{frustration}} = 1 - \rho^3 > 1$$

which happens to be true in the interval $-1 \leq \rho < 0$. This proves that any order parameter is unstable to paramagnetic perturbations. This leaves no room for other stable order parameters than the trivial paramagnetic one, concluding our proof.

- [1] G. P. M. Mézard and M. Virasoro, *Spin Glass Theory and Beyond* (World Scientific, Singapore, 1987).
- [2] L. Viana and A. J. Bray, *J. Phys. C* **18**, 3037 (1985).
- [3] G. Parisi, *Phys. Lett. A* **73**, 203 (1979).
- [4] G. Parisi, *Phys. Rev. Lett.* **50**, 1946 (1983).
- [5] C. DeDominicis and Y. Y. Goldschmidt, *Journal of Physics A Mathematical General* **22**, L775 (1989).
- [6] M. Mézard and R. Zecchina, *Phys. Rev. E* **66**, 056126 (2002).
- [7] R. Mulet, A. Pagnani, M. Weigt, and R. Zecchina, *Phys. Rev. Lett.* **89**, 268701 (2002).
- [8] M. Mézard and G. Parisi, *J. phys* **47**, 1285 (1986).
- [9] M. Weigt and A. K. Hartmann, *Phys. Rev. Lett.* **84**, 6118 (2000).
- [10] M. Weigt and A. K. Hartmann, *J. Phys. A* **36**, 11096 (2003).
- [11] M. Mézard and G. Parisi, *The European Physical Journal B* **20**, 217 (2001).
- [12] M. Mézard and G. Parisi, *Journal of Statistical Physics* **111**, 1 (2003).
- [13] M. Mézard, G. Parisi, and M. Virasoro, *Europhys. Lett.* **1**, 77 (1986).
- [14] R. Z. O.C. Martin, R. Monasson, *Theoretical Computer Science* **265**, 3 (2001).
- [15] F. Krzakala, A. Montanari, F. Ricci-Tersenghi, G. Semerjian, and L. Zdeborová, *Proc. Nat. Acad. Sci.* **104**, 10318 (2007).
- [16] F. Krzakala and L. Zdeborová, *Phys. Rev. E* **76**, 031131 (2007), arXiv.org:cond-mat/0704.1269v2.
- [17] M. Mézard, G. Parisi, and R. Zecchina, *The European Physical Journal B* **297**, 812 (2002).
- [18] A. Braunstein, R. Mulet, A. Pagnani, M. Weigt, and R. Zecchina, *Phys. Rev. E* **68**, 036702 (2003).
- [19] H. Zhou, *The European Physical Journal B* **32**, 265 (2003).
- [20] J. Yedidia, W. T. Freeman, and Y. Weiss, *IT-IEEE* **51**, 2282 (2005).
- [21] A. Montanari and T. Rizzo, *Journal of Statistical Mechanics: Theory and Experiment* **2005**, P10011 (2005).
- [22] M. Chertkov and V. Y. Chernyak, *Physical Review E* **73**, 065102 (2006), arXiv.org:cond-mat/0601487.
- [23] M. Chertkov and V. Y. Chernyak, *Journal of Statistical Mechanics: Theory and Experiment* **2006**, P06009 (2006).
- [24] E. Marinari, F. Parisi, G. Ricci-Tersenghi, J. Ruiz-Lorenzo, and F. Zuliani, *Journal of Statistical Physics* **98**, 973 (2000).
- [25] C. M. Newman and D. L. Stein (2005), arXiv.org:cond-mat/0503345.
- [26] M. Ostilli, F. Mukhamedov, and J. F. F. Mendes (2006), arXiv.org:cond-mat/0611654.
- [27] F. R. Kschischang, B. J. Fret, and H.-A. Loeliger, *IEEE Transf. Inf. Theory* **47**, 498 (2001).
- [28] T. Castellani, F. Krzakala, and F. Ricci-Tersenghi, *The European Physical Journal B* **47**, 99 (2005), arXiv.org:cond-mat/0403053.
- [29] A. Montanari and F. Ricci-Tersenghi, *European Physical Journal B* **51**, 339 (2003).
- [30] L. Dall'Asta, A. Ramezanpour, and R. Zecchina (2008), arXiv.org:cond-mat/0801.2890.